ABSTRACT

Targeting Tumor Hypoxia with Small-Molecule Anticancer Agents

Evelyn D. Le

Director: Kevin G. Pinney, Ph.D.

A vascular network delivers nutrients and oxygen to solid tumors, therefore selectively targeting tumor vasculature with anticancer agents represents a potentially promising therapeutic strategy. Small-molecule anticancer compounds that interact at the colchicine-binding site on beta-tubulin and inhibit microtubule formation can function as cytotoxic agents. In addition, a sub-set of these inhibitors of tubulin polymerization selectively disrupt blood flow to tumors and are referred to as vascular disrupting agents (VDAs). Through their ability to inhibit tubulin polymerization, VDAs induce morphology changes in the endothelial cells lining tumor vasculature, leading to vessel damage and ultimately precluding blood flow to the tumor. A variety of solid tumor cancers contain pronounced regions of low oxygen (hypoxia). In order to selectively target tumor hypoxia, small-molecule tubulin-binding agents (both antiproliferative agents and VDAs) can be synthetically linked to bioreductive triggers such as monomethyl or dimethyl nitrothiophenes, forming bioreductively activatable prodrug conjugates (BAPCs) that are designed to selectively release the anticancer agent in regions of hypoxia. The natural product combretastatin A-1 (CA1) and a synthetic analogue, phenstatin, are potent inhibitors of tubulin polymerization ($IC_{50} = 1.9$ μM and 1.0 μM, respectively) and CA1 functions as a VDA. The focus of this study centers on the synthesis of CA1 BAPCs that incorporate a monomethyl trigger and a phenstatin BAPC bearing a dimethyl trigger.

APPROVED BY DIRECTOR OF HONORS THESIS:

_____

Dr. Kevin G. Pinney, Department of Chemistry and Biochemistry

APPROVED BY THE HONORS PROGRAM

_____

Dr. Elizabeth Corey, Director

DATE:_____

TARGETING TUMOR HYPOXIA WITH SMALL-MOLECULE

ANTICANCER AGENTS

A Thesis Submitted to the Faculty of

Baylor University

In Partial Fulfillment of the Requirements for the

Honors Program

By

Evelyn D. Le

Waco, Texas

May, 2016

TABLE OF CONTENTS

TABLE OF FIGURES

TABLE OF SCHEMES

TABLE OF ABBREVIATIONS

AIA   Angiogenesis Inhibiting Agent

AML   Acute Myelogeneous Leukemia

BAPC   Bioreductively Activatable Prodrug Conjugate

CA1   Combretastatin A-1

CA1P   Combretastatin A-1 Phosphate

CA4   Combretastatin A-4

CA4P   Combretastatin A-4 Phosphate

CIS   Cisplatin

Cyt P450   Cytochrome P450

DNA   Deoxyribonucleic Acid

FAK   Focal Adhesion Kinase

G2/M   Gap 2/ Mitosis

GI_{50} 50% Growth Inhibition

IC_{50} 50% Inhibitory Concentration

MDS   Myelodysplastic Syndromes

MLC	Myosin Light Chain
MP	Myosin Light Chain Phosphatase
RhoA-GDP	RhoA- Guanidine Diphosphatase
RhoA-GTP	RhoA- Guanidine Triphosphatase
ROCK	Rho Kinase
SAR	Structure Activity Relationship
SRB	Sulforhodamine B
TPZ	Tirapazamine
VDA	Vascular Disrupting Agent
VEGF	Vascular Endothelial Growth Factor
VTA	Vascular Targeting Agent

ACKNOWLEDGEMENTS

I would like to thank my thesis advisor Dr. Kevin G. Pinney for guiding me throughout

the whole process. I also would like to thank Blake A. Winn, the graduate student in the

Pinney Group for inspiring me about the cancer research and teaching me the lab

techniques.

CHAPTER ONE

Introduction

The Vascular Network of Tumor Tissue

A normal, healthy vascular network is hierarchically organized, and driven by metabolic demand and blood supply (Figure 1).[1] Tumors are proficient in recruiting a sufficient blood supply to support their pronounced growth. Therefore, the vasculature that feeds tumors forms rapidly and tends to be inherently unstable and disorganized. The blood vessels including arterioles, capillaries, and venules are inconsistent in shape and diameter. Thus, nutrients are not delivered sufficiently and waste products are not removed via the lymphatic system effectively. The unique characteristics of tumor vasculature create new opportunities for selective vascular targeting strategies.[1]
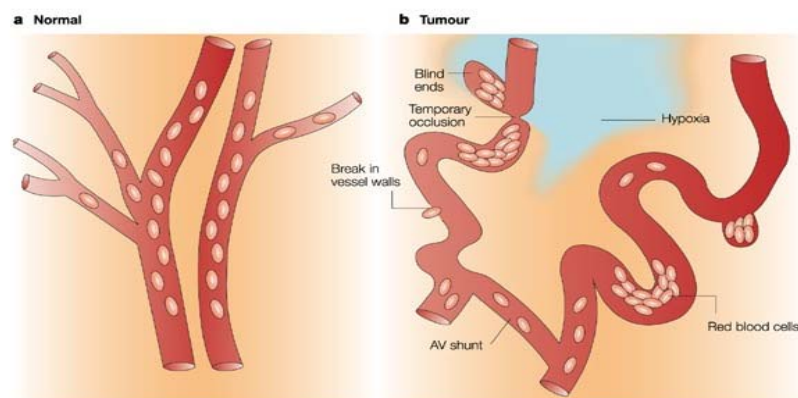

Figure 1: The vascular network of normal tissue versus tumor tissue [directly reproduced from reference 2].[2]

Vascular targeting agents (VTAs) are divided into two groups: angiogenesis inhibiting agents (AIAs) and vascular disrupting agents (VDAs) (Figure 2).[3–5] Their mechanisms of action are very distinct. The AIAs inhibit the formation of new vessels while the VDAs destroy existing tumor vasculature.[3] An example of an AIA is bevacizumab (Avastin[TM]), which is a recombinant humanized monoclonal antibody.[6] Bevacizumab binds to vascular endothelial growth factor (VEGF) and inhibits the interaction between VEGF and its corresponding receptors.[5] The mechanism of small molecule VDAs involves the interaction with the tubulin-microtubule protein systems.[7]
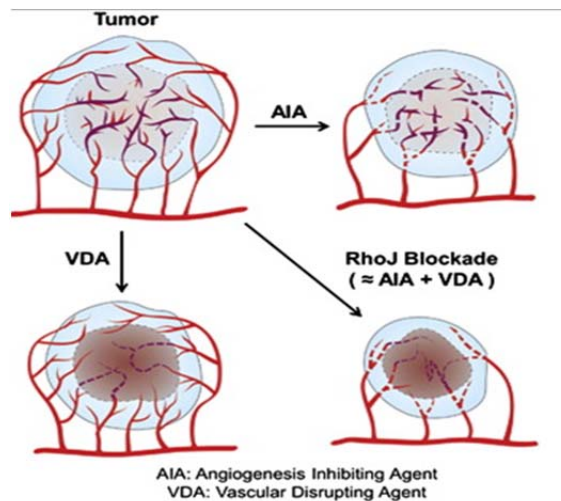

Figure 2: AIA and VDA [directly reproduced from reference 8].[8]

The tubulin-microtubule protein system has several small-molecule binding sites such as vinca alkaloid, colchicine, taxoid binding domain on the microtubule, etc.[9] They are located on the αβ- tubulin heterodimer and interact with a binding domain on the microtubule.[7] Microtubule-destabilizing agents, which inhibit microtubule polymerization, bind to either vinca alkaloid or colchicine binding sites.[10] Microtubule-stabilizing agents, which enhance microtubule polymerization, bind to taxoid binding domain.[11] This study centers on combretstatin, which is one of the microtubule-destabilizing VDAs.

The mechanism by which VDAs induce changes in the endothelial morphology of cells is by binding to the colchicine site on β-tubulin. VDAs disrupt mitotic spindles, induce cell cycle arrest at G2/M stage of the cell cycle and promote cell death.[12] Even though arrested cells may escape from the spindle checkpoints, this event results in abnormal chromatid segregation, followed by cell death.[12] As a result, microtubule disassembly leads to cell rounding and detachment, resulting in a rapid collapse in tumor blood flow.[13]

In their collaborative (Pinney and Trawick Groups Baylor University) 2016 article, these researchers proposed a mechanism of VDA's effects on the endothelial cells.[14] As depicted in Figure 3, a phosphatase enzyme will cleave the phosphate from an inactive VDA prodrug, resulting in a release of the active VDA. Once the active VDAs enter the endothelial cell membrane via simple diffusion, they bind to the colchicine site on the tubulin heterodimer and prevent microtubule formation.[14] As a result, tubulin

3

depolymerization occurs and subsequently, a guanidine diphosphatase (RhoA-GDP) is phosphorylated into a guanidine triphosphatase (RhoA-GTP) that activates Rho kinase (ROCK) and regulates a cytoskeleton reorganization. This includes an increase in cell contractility, formation of focal adhesion and membrane blebbing.[15,16] ROCK has three routes of effect that occur simultaneously. Via a FAK pathway, ROCK phosphorylates the super assemblies of integrins, cytoskeletal and signaling proteins such as talin, α-actinin, vinculin, paxilin, and focal adhesion kinase (FAK), increasing a focal adhesion formation and an actin-myosin contractility, leading to a significant detachment of endothelial cells.[17,18] ROCK also phosphorylates a myosin light chain (MLC), which directly activates actin bundling, stress fiber formation, cell-extracellular matrix interactions, and disrupts cell-cell junctions, resulting in an increase in permeability.[19] At the same time, ROCK inactivates the MLC phosphatase (MP), leading to the same effects.[20]
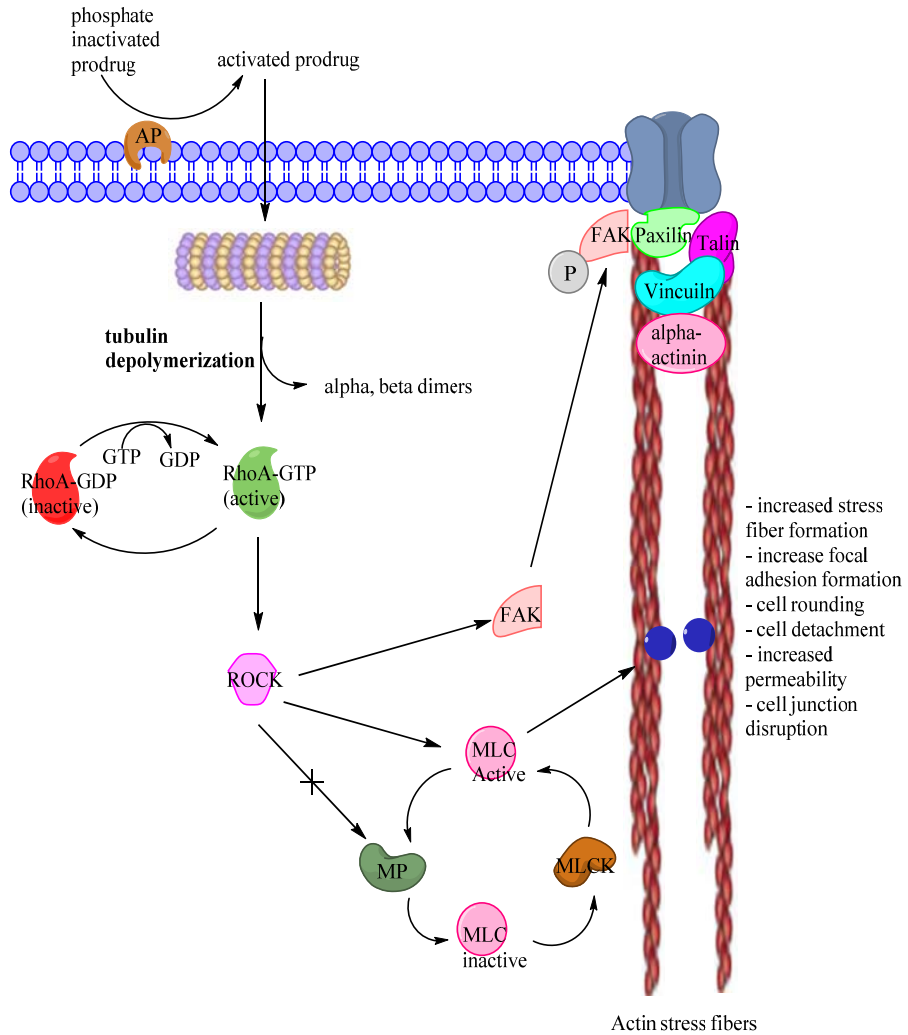
Figure 3: Proposed mechanism of action of VDA prodrug in activated endothelial cells [directly reproduced from reference 14]. [14]

In the article published in 2005 by the Tozer group, they proposed a mechnism of action of the small molecule VDAs, which changes the endothelial cells into a blebbing shape.[21] In vivo, this would increase the "vascular resistance to blood flow,"[21] causing an increase in tumor vascular permeability and protein leakage.[21] The leakage results in a retention of fluid, which generates a high interstitial fluid pressure upon the vasculature, causing active vasoconstriction and vascular shutdown.[21]

Figure 4: Proposed mechanism of rapid tumor vascular shutdown after treatment with VDAs [directly reproduced from reference 21]. [21]

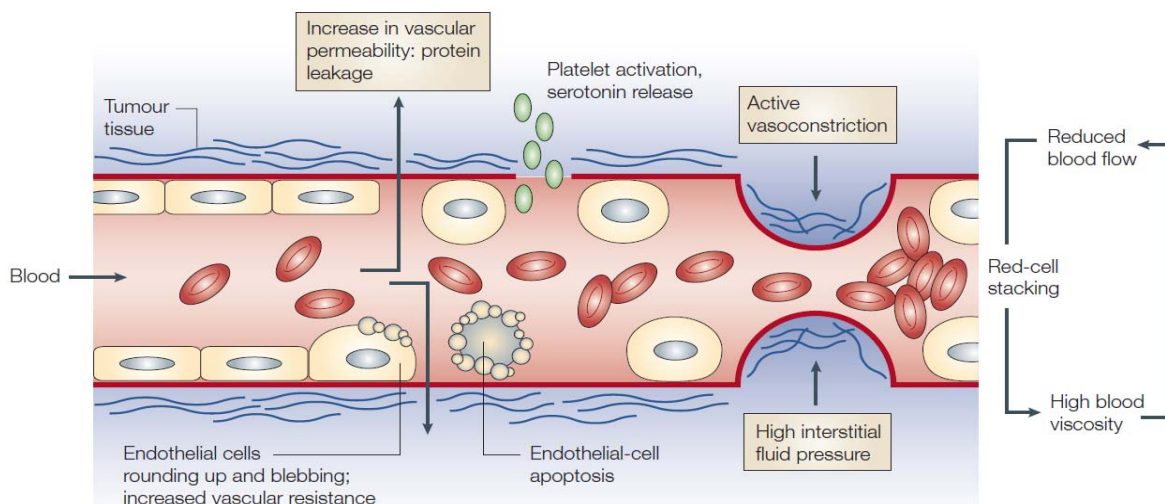In short, small molecule VDAs inhibit the assembly of tubulin into microtubules at the colchicine binding site of tubulin, leading to microtubule depolymerization that results in cell retraction, rounding and detachment.[5] Without sufficient oxygen and nutrients, the vascular damage due to VDA treatment leads to cell death.[5]

Targeting Hypoxia and Bioreductively Activatable Prodrug Conjugates

Small-molecule tubulin-binding VDAs can be synthetically linked to bioreductive triggers, forming bioreductively activatable prodrug conjugates (BAPCs) that are designed to selectively release the anticancer agent in the hypoxic regions.[22] Bioreductive prodrugs are biologically inactive molecules that use enzymatic reduction to convert to an active form.[23] Enzymatic reduction mechanisms can involve a one-electron reduction or a

two-electron reduction.[22] One electron reductases catalyze an oxygen-sensitive activation of bioreductive prodrugs in which one electron reductases generate prodrug free radical species under hypoxic conditions.[24] They then can undergo further fragmentaion and disproportionation and become cytotoxic agents.[24] Under normoxic conditions however, due to the redox cycle, the free radical species can reoxidize back to their parent compound and generate superoxide radicals.[25] Thus, no futher fragmentation or cytotoxic agents can occur. The two-electron reductase bypasses the formation of an intemediate radical prodrug step, leading to a formation of active toxic drug.[25] This irreversible pathway catalyzes an insensitive oxygen activation of bioreductive prodrugs.[24] There are numerous chemical classes of BAPCs including: nitro groups, quinones, aromatic N-oxides, aliphatic N-oxides and transition metals.[22]

Clinical Experience of VDAs

PR-104, is the first hypoxia-activated prodrug compound that entered clinical trials.[26] It has currently undergone a phase I/II study experimenting on leukemia[27] and is still active in clinical trials.[22,25] Its mechanism of action involves the one-electron reductase enzyme known as NADPH:cytochrome P450 oxidoreductase (P450), which catalyzes the transfer of electrons to microsomal cytochrome P450.[28] The endogenous nitroreductases [Figure 5] in the tumor activate the reactive center of PR-104, producing an oxygen-sensitive free radical intermediate, thus generating an activated nitrogen mustard that has more reactive leaving groups such as bromide and mesylate.[29] PR-104 prodrug functions as a hypoxia-selective DNA cross-linking agent.
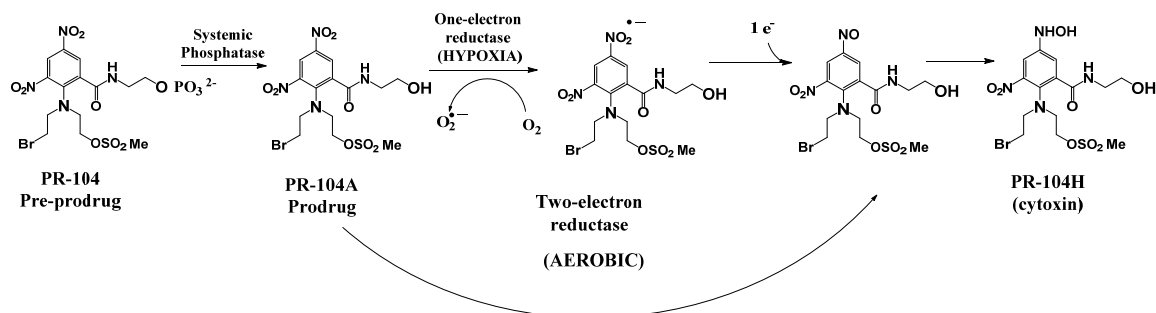
Figure 5: Mechanism of action of PR-104 [directly reproduced from reference 30].[30]

Tirapazamine is a bioreductive prodrug, which belongs to the aromatic N-oxide chemical class.[22] In Figure 6, the one-electron reductase activates tirapazamine and split it into one of two active radical forms.[31] The trigger becomes a Michael acceptor, which binds to nucleophilic bases, damaging DNA by breaking its double strand.[32] In 2010, the Kenny Group (Peter MacCallum Cancer Center, Australia) conducted a phase III clinical trial study of tirapazamine (TPZ), cisplatin (CIS), and radiation versus cisplatin and radiation of advanced head and neck cancer cells over 2 years.[33] The study recruited patients from 89 sites in 16 countries and used a randomized trial.[27] As a result, there is no evidence that shows a significant improvement when adding tirapazamine to cisplatin and radiation (65.7% for CIS and 66.2% for TPZ/CIS).[33] Therefore, its current clinical status is closed.[22]
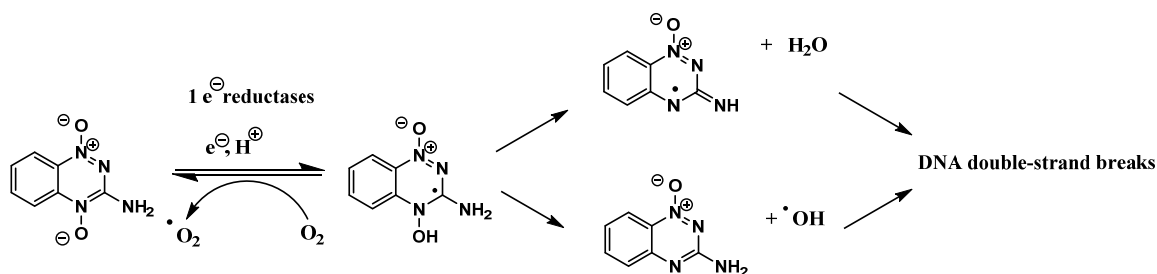

Figure 6: Mechanism of action of Tirapazamine [directly reproduced from reference 31].[31]

8

Combretastatin A-1 (CA1)[34] and combretastatin A-4 (CA4)[35] [Fig. 7] are both natural products that are isolated from the South African tree *Combretum caffrum*. They are both strong inhibitors of tubulin polymerization that can be synthetically linked to bioreductive triggers, forming BAPCs.[36] CA1 and CA4 share nearly identical stillbene structures except that CA1 has an additional hydroxyl group at the C-2' position.[37] A monophosphate group attached to the C-3' position of CA4 has proven to be water soluble (referred to as CA4P); and morover successful in phase I clinical trials.[38] In 2015, OXiGENE has announced that CA4P will undergo phase II/III randomized studies in ovarian cancer. As a result, the study will be started in May, 2016 focussing on PCC/bevacizumab/CA4P against PCC/bevacizumab/placebo, in which phase II recruits 80 subjects and phase III recruits 356 subjects.[39] Meanwhile, a water-soluble diphosphate prodrug derivative of CA1 (referred to as CA1P) has undergone phase I clinical trials experimenting on acute myelogeneous leukemia (AML), myelodysplastic syndromes (MDS) and hepatic tumors.[40,41]

Structure activity relationship (SAR) studies related to CA4 analogues and derivatives led to an effort to prepare an epoxide moiety as a replacement for the ethylene bridge. Interestingly, a Jacobsen epoxidation reaction did not yield the intended CA4-epoxide bur rather formed an interesting diaryl ketone referred to as phenstatin.[42] The epoxide of CA4 was eventually prepared by sulfur ylide mediated epoxiation of silyl-protected isovanillin.[43] This new vascular discrupting agent was synthesized by the Pettit group in 1998.[42] Phenstatin and phenstatin prodrug have not yet entered clinical trials.
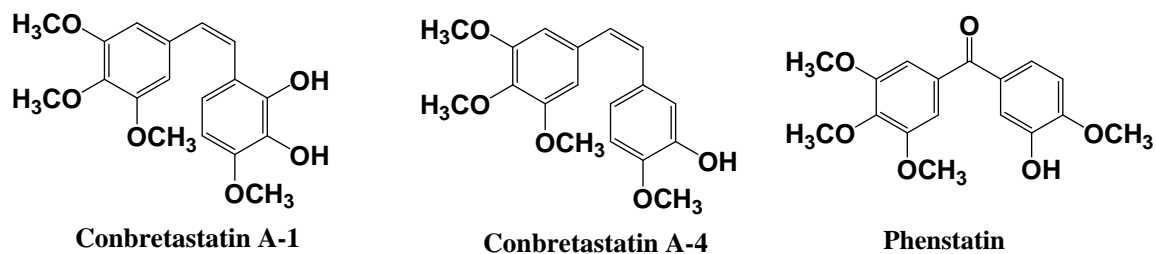
Figure 7: Combretastatin A-1 [34], combretastatin A-4 [35] , phenstatin [44]

The sulforhodamine B (SRB) assay is used for cytotoxicity determination, including GI_{50} values at 50% growth inhibition and IC_{50} values at 50% inhibitory concentration, based on the measurement of cellular protein content. Compounds are adherent to a 96-well format and incubated. The monolayer is fixed with 10% trichloroacetic acid and stained for 30 minutes. 10 mM Tris base is used to dissolve the protein-bound dye. The excess dye is washed by 1% acetic acid. A microplate reader is used to determine the cytotoxicity at 510nm.[45]

Cytotoxicity (GI_{50} values at 50% growth inhibition) of the three stilbenes in three different cancer cell lines (Table 1), ranks them from highest to lowest as CA1, phenstatin, and CA4 respectively.[42,46] In order to achieve 50% reduction in proliferation of cancer cell growth, a higher concentration of CA1 is needed to achieve the same result as phenstatin and CA4 at lower concentrations. Thus, CA4 is better than CA1 and phenstatin in term of 50% reduction of proliferation of cancer cell growth.[42]

CA4 and phenstatin (Table 2) have almost equivalent effectiveness in inhibiting the tubulin polymerization (IC_{50} = 1.2 μM and 1.0 μM, respectively), which are better than CA1 (IC_{50} = 1.9 μM).[42,46,47]

	GI$_{50}$ (nM) DU-145 Prostate	GI$_{50}$ (nM) SK-OV-3 Ovarian	GI$_{50}$ (nM) NCI-H460 Lung
CA4[a]	6.02 ± 0.66	5.06 ± 0.145	5.00 ± 0.359
CA1[a]	33.0 ± 17.3	38.4 ± 24.2	15.3 ± 15.8
Phenstatin[b]	ND	10.4	17.9

Table 1: SRB cytotoxicity assay data for combretastatin A-1, combretastatin A-4, and

phenstatin against human cancer cell lines [DU-145 (prostate), SK-OV-3 (ovarian), and

NCI-H460 (lung)]

[a] Data from Ref. 44

[b] Data from Ref. 40

	Combretastatin A-4[a]	Combretastatin A-1[b]	Phenstatin[c]
IC$_{50}$ (µM) ± SD Tubulin polymerization inhibition	1.2 ± 0.1	1.9	1.0 ± 0.2

Table 2: Inhibition of tubulin polymerization of combretastatin A-1, combretastatin A-4,

and phenstatin.

[a] Data from Ref. 44

[b] Data from Ref. 45

[c] Data from Ref. 40

Bioreductive Nitrothiophene Triggers

In 2006, Peter Davis and co-workers synthesized three nitropthiophene triggers

that were synthetically attached to CA4.[48] The geminal dimethyl trigger (Figure 8) was

the most effective because it displayed the most resistance to aerobic metabolism.[48] This means that CA4 with the trigger attached would target the hypoxic region specifically without affecting the normal oxygen environment or other related normal cells.[48] Moreover, the sterically bulky geminal methyl groups helped stabilize the compounds without releasing the anti-cancer agent early due to enzymatic processes.[48] Furthermore, less metabolic oxidation occured due to a lack of a hydrogen atom at the α position to the aromatic group.[48] The normethyl trigger has two hydrogens at the α position and the monomethyl trigger has one while the geminal dimethyl has none. Different range of oxigen (hypoxia or normoxia) would oxidize the hydrogen and cleave the drug. Thus, the CA4 with geminal dimethyl or monomethyl triggers attached would not likely cleave in different range of oxygen.[48]

*nor*methyl   *mono*methyl   *di*methyl
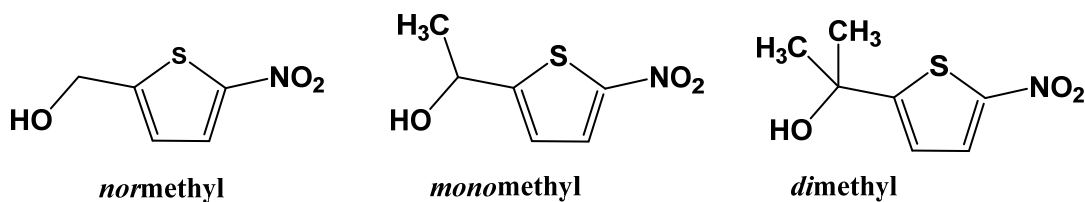
Figure 8: Nitrothiophene triggers [directly reproduced from reference 48]. [48]

The reduction mechanism (Fig 9) for CA4 with the *geminal-di*methyl nitrothiophene trigger attached was carried out via cytochrome P450 reductase, releasing the active CA4.[48] Thus, the CA4 BAPC functions as an inactivated produg that needs the Cyt P450 reductase to activate and cleave off the trigger to release CA4. CA4 becomes an active agent that goes through the signal pathways as described in Figure 3 and 4.
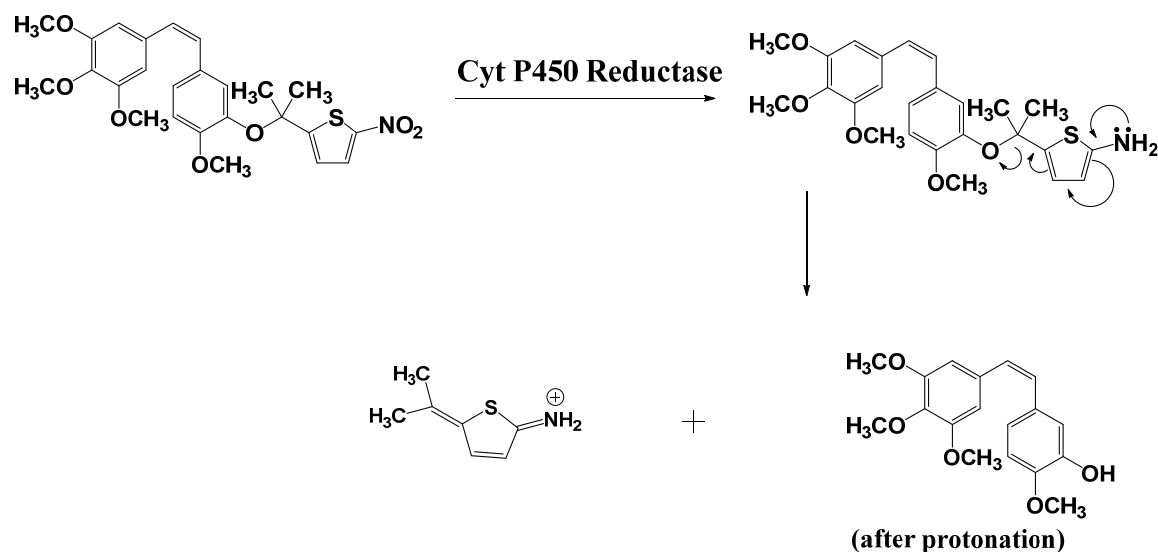
Figure 9: CA4 BAPC reduction mechanism [directly reproduced from reference 48].[48]

The general concept in this study is taking potent inhibitors of tubulin polymerization and preparing them as BAPCs to selectively target hypoxia. Particularly, in this study, a selective protection strategy is used to synthesize CA1 based on the work from the Pinney Group (Baylor University)[49,50] in order to attach the synthesized *mono*methyl nitrothiophene trigger to the C-2 or C-3 position. The synthesis of phenstatin will also be performed in order to attach the *geminal-di*methyl nitrothiophene trigger to the C-3 position.

13

CHAPTER TWO

Results and Discussions

Scheme 1 focuses on the synthesis of the nitrothienyl bioreductive triggers. Scheme 2 highlights the synthesis of protected CA1 analogs using the Wittig reaction, which produced both E- and Z- isomers, but favors the Z-isomer of CA1.[30, 31] Scheme 3 displays the synthesis of phenstatin analogs.

Scheme 1: Synthesis of Nitrothiophene Bioreductive Triggers [48]
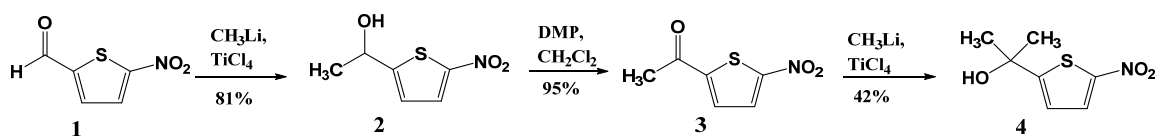
The *mono*-methyl trigger **2** was generated by reacting ketone **1** with methyl lithium (CH$_3$Li) and titanium tetrachloride (TiCl$_4$) in diethyl ether.[48] The *mono*-methyl trigger was then oxidized using Dess-Martin Oxidation (DMP) in dichloromethane to yield **3**. The resultant ketone 3 was methylated using methyl lithium (CH$_3$Li) and titanium tetrachloride (TiCl$_4$) in diethyl ether to yield *gem*-dimethyl thiophene **4**.[48]

Scheme 2: Synthesis of CA1 BAPCs [49,50]
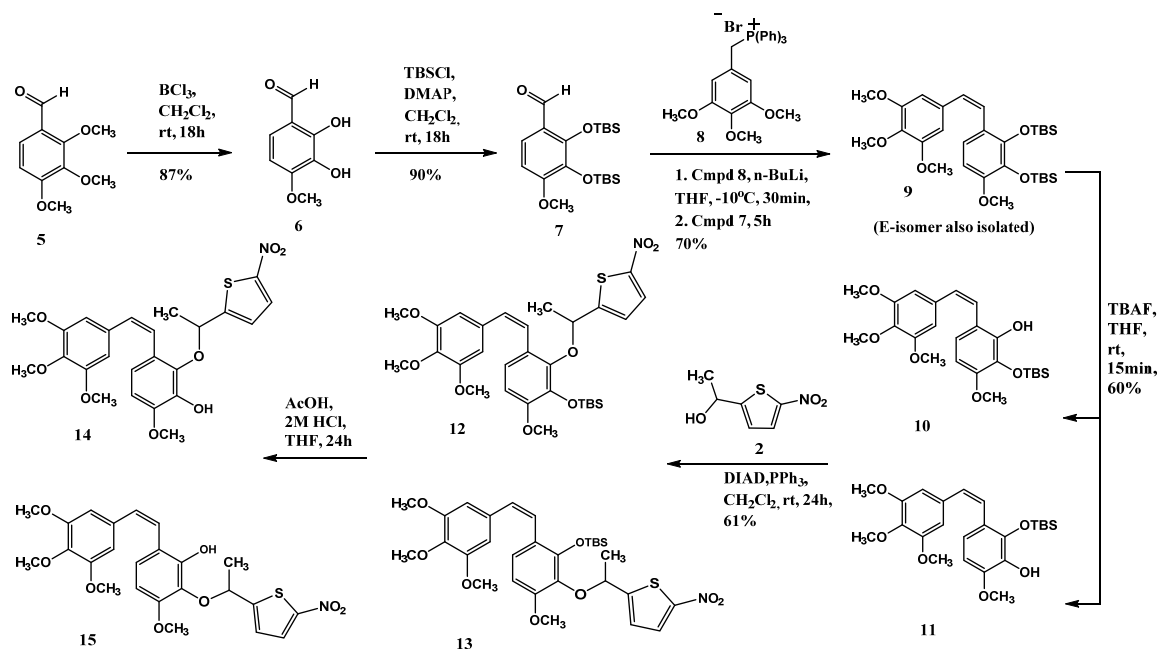
The *tert*-butyldimethylsilyl ether (TBS) protecting group was used to synthesize the mono-trigger CA1, as shown in scheme 2.[50] Boron chloride was used to selectively demethylate the aldehyde **5** to generate the diol required for CA1, yielding aldehyde **6**.[49,50] Only the C-2 and C-3 methyl groups are cleaved, leaving C-4 methoxy unchanged.[30,31] TBS groups were used to protect the phenolic alcohols of aldehyde **6** by treatment with triethylamine (Et$_3$N), 4-dimethylaminopyridine (DMAP), and two equivalents of TBSCl to generate aldehyde **7**.[49,50] Phosphonium salt **8** in the Wittig reaction was used to react with aldehyde **7** to produce the Z- and E- isomers **9**, favoring the Z-isomer.[49] The stillbene **9** was deprotected using tetra-*N*-butylammonium fluoride (TBAF), yielding mono-protected stillbene **10** at C-2 and **11** at C-3.[49] Stillbene **10** or **11**, *mono*-methyl trigger **2**, and triphenylphosphine were mixed using a Mitsunobu reaction to generate CA1 *mono*-methyl BAPC **12** or **13**.[49] Acetic acid (AcOH) and hydrochloric acid (HCl) were used to deprotect CA1 *mono*-methyl BAPC **14** and **15**.[49]

15

Scheme 3: Synthesis of Phenstatin BAPCs [35]
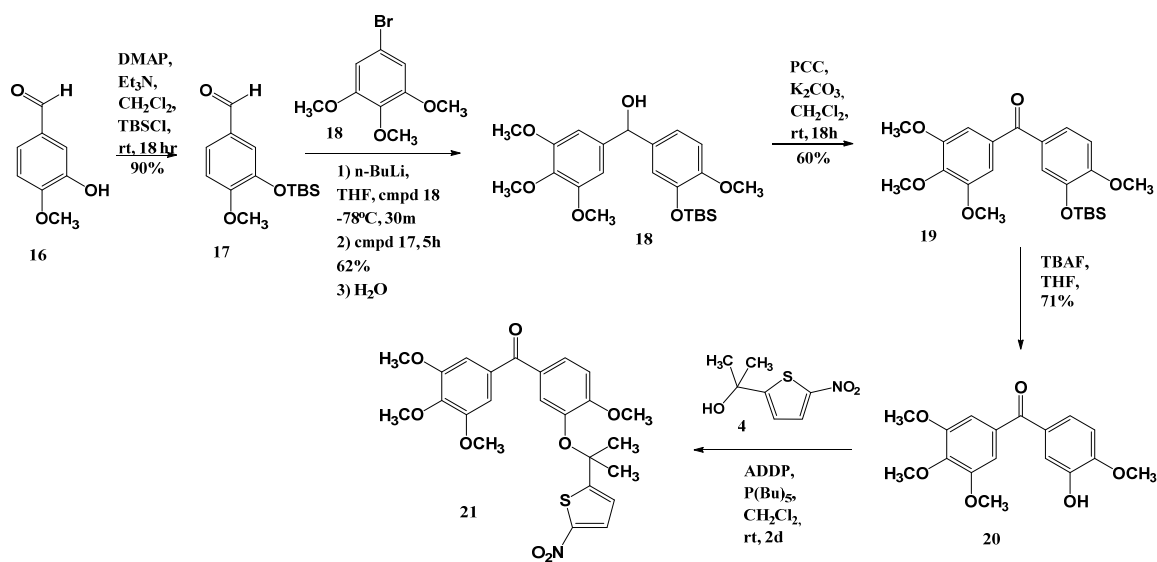
The synthetic route for the phenstatin BAPCs is illustrated in Scheme 3.[35] Isovanilin 1**6** was reacted with TBSCl, DMAP, and Et₃N to form a protected aldehyde **17**.[35] The secondary alcohol **19** was formed by reacting the protected aldehyde **17** into a halogen-metal exchange with compound **18**.[35] The alcohol **19** was oxidized to the ketone **20** using pyridinium chlorochromate (PCC) and K_2CO_3.[35] TBAF was used to deprotect the ketone **20,** yielding phenstatin **21.** The phenstatin-*gem-di*methyl BAPC **22** was formed by mixing phenstatin **21**, *geminal-di*methyl trigger **3**, ADDP, tributylphosphine in the Mitsunobu reaction.[35]

CHAPTER THREE

Experimental Sections

General Experimental Procedures.[49,50] Dichloromethane [CH_2Cl_2] and tetrahydrofuran [THF] were used in their anhydrous forms. Reactions were, unless specified, performed under an inert atmosphere using nitrogen gas. Thin-layer chromatography (TLC) plates (precoated glass plates with silica gel 60 F254, 0.25 mm thickness) were used to monitor reactions. Purification of intermediates and products were carried out with a flash purification system using silica gel (200-400 mesh, 60 Å) or RP-18 prepacked columns. Intermediates and products synthesized were characterized on the basis of their ^{1}H NMR (500 MHz) and ^{13}C NMR (125 MHz) spectroscopic data. TMS was used as an internal standard for spectra recorded in $CDCl_3$. All the chemical shifts are expressed in ppm (δ), coupling constants (J) are presented in Hz, and peak patterns are reported as broad (br), singlet (s), doublet (d), doublet of doublets (dd) triplet (t), quartet (q), septet (sept), and multiplet (m). Purity of the final compounds was further analyzed at 25 °C using an Agilent 1200 HPLC system with a diode-array detector (λ = 190-400 nm), a Zorbax XDB-C18 HPLC column (4.6 mm x 150 mm, 5 μm), and a Zorbax reliance cartridge guard-column; eluents, solvent A, 0.1% TFA in H_2O, solvent B, 0.08% TFA in acetonitrile-H_2O (80:20 (v/v) ratio); gradient, 80% A/20% B over 0 to 5 min; 80% A/20% Bf5% A/ 95% B over 5 to 35 min; 5% A/95% B over 35 to 45 min; post-time 15 min; flow rate 1.0 mL/min; injection volume 20 μL; monitored at wavelengths of 254, 264, 280, and 300 nm. [Note: 4-dimethylaminopyridine is abbreviated DMAP, sodium bicarbonate is abbreviate $NaHCO_3$, hydrochloric acid is abbreviated HCl, ethyl acetate is

abbreviated EtOAc, N,N-dimethylformamide is abbreviated DMF, chloroform-d is abbreviated CDCl$_3$]

1-(5-Nitrothiophen-2-yl)ethanol (2):[32] In a dry ice bath at -78°C, TiCl$_4$ (1.84 mL) was added dropwise in diethyl ether (70 mL). CH$_3$Li (10.4 mL) was subsequently added dropwise to the solution and the reaction mixture was stirred for 1.5 h. 5-Nitrothiophene-2-carboxaldehyde (**1**) (1.900 g, 12.09 mmol) was dissolved in Et$_2$O (140 mL) and the solution was added dropwise to the previous TiCl$_4$, CH$_3$Li, and diethyl ether reaction using a drop funnel. The reaction was subsequently stirred for 12 h. The solution was then extracted with ethyl acetate, dried with sodium sulfate, and evaporated under reduced pressure. Flash chromatography of the crude product using a prepacked 100 g silica column [eluents: solvent A, EtOAc; solvent B, hexanes; gradient, 10% A/90% B over 1.19 min (1 CV), 10% A/90% B → 64% A/36% B over 13.12 min (10 CV), 64% A/36% B over 2.38 min (2 CV); flow rate 100.0 mL/min; monitored at λ 254 and 280 nm] yielded 1-(5-nitrothiophen-2-yl)ethanol (**2**) (0.932 g, 5.38 mmol, 81%) as a brown oil, ^{1}H NMR (500 MHz, CDCl$_3$) δ 7.81 (1H, d, J = 4 Hz), 6.90 (1H, d, J = 4 Hz), 5.15 (1H, dq, J = 6 Hz, J = 5 Hz), 2.23 (1H, d, J = 5 Hz), 1.63 (3H, d, J = 6 Hz). ^{13}C NMR (125 MHz, CDCl$_3$) δ 160.0, 149.9, 129.1, 122.2, 66.3, 25.1.

2-Acetyl-5-nitrothiophene (3):[32] 1-(5-Nitrothiophen-2-yl)ethanol (**2**) (4.700 g, 27.11 mmol) was dissolved in CH$_2$Cl$_2$ (240 mL). DMP (14.20 g, 33.48 mmol) was added to the reaction, which was subsequently stirred for 1 h. The reaction was then quenched with saturated Na$_2$S$_2$O$_3$, then further quenched with NaHCO$_3$. The solution was extracted with

ethyl acetate (3 x 30 mL), washed with 2 x H_2O/brine, dried with Ns_2SO_4, and evaporated under reduced pressure. Flash chromatography of the crude product using a prepacked 100 g silica column [eluents: solvent A, EtOAc; solvent B, hexanes; gradient, 10% A/90% B over 1.19 min (1 CV), 10% A/90% B → 80% A/20% B over 13.12 min (10 CV), 80% A/20% B over 2.38 min (2 CV); flow rate 100.0 mL/min; monitored at λ 254 and 280 nm] yielded 2-Acetyl-5-nitrothiophene (**3**) (4.437 g, 25.75 mmol, 95%) as a brown oil, ^{1}H NMR (500 MHz, $CDCl_3$) δ 7.81 (1H, d, J = 4 Hz), 6.90 (1H, d, J = 4 Hz), 5.15 (1H, dq, J = 6 Hz, J = 5 Hz), 2.23 (1H, d, J = 5 Hz), 1.63 (3H, d, J = 6 Hz). ^{13}C NMR (125 MHz, $CDCl_3$) δ 160.0, 149.9, 129.1, 122.2, 66.3, 25.1.

2-(5-Nitrothien-2-yl)Propan-2-ol (4):[32] In a dry ice bath at -78°C, $TiCl_4$ (1.84 mL) was added dropwise in diethyl ether (70 mL). CH_3Li (10.4 mL) was then added dropwise to the solution, which was subsequently stirred for 1.5 h. 2-Acetyl-5-nitrothiophene (**3**) (1.900 g, 11.02 mmol) was dissolved in Et_2O (140 mL) and the solution was added dropwise to the previous $TiCl_4$, CH_3Li, and diethyl ether reaction using a drop funnel. The reaction was subsequently stirred for 12 h. The solution was then extracted with ethyl acetate, dried with sodium sulfate, and evaporated under reduced pressure. Flash chromatography of the crude product using a prepacked 100 g silica column [eluents: solvent A, EtOAc; solvent B, hexanes; gradient, 10% A/90% B over 1.19 min (1 CV), 10% A/90% B → 80% A/20% B over 13.12 min (10 CV), 80% A/20% B over 2.38 min (2 CV); flow rate 100.0 mL/min; monitored at λ 254 and 280 nm] yielded 1-(5-Nitrothiophen-2-yl)Propan-2-ol (**4**) (2.037 g, 10.82 mmol, 42%) as a brown oil, ^{1}H NMR

(60 MHz, CDCl$_3$) $^\delta$ 1.67 (s, 6H), 2.1 (br, 1H), 6.88 (d, J = 4 Hz, 1H), 7.8 (d, J = 4 Hz, 1H) ppm.

2,3-Dihydroxy-4-methoxybenzaldehyde (**6**):[49,50] 2,3,4-Trimethoxybenzaldehyde (**5**) (4.000 g, 20.30 mmol) was added to dry CH$_2$Cl$_2$ (80 mL) in a 0°C ice bath. Boron trichloride (45 mL, 45 mmol, 1.0 M) was added dropwise to the reaction and the solution was stirred for 18 h. The reaction was then quenched with NaHCO$_3$ and acidified with HCl to pH 2. Ethyl acetate was used to extract the product, which was then dried with sodium sulfate, and evaporated under reduced pressure. Flash chromatography of the crude product using a prepacked 100 g silica column [eluents: solvent A, EtOAc; solvent B, hexanes; gradient, 10% A/90% B over 1.19 min (1 CV), 10% A/90% B → 69% A/31% B over 13.12 min (10 CV), 69% A/31% B over 2.38 min (2 CV); flow rate 50.0 mL/min; monitored at λ 254 and 280 nm] yielded 2,3-dihydroxy-4-methoxybenzaldehyde (**6**) (2.64 g, 15.7 mmol, 87%) as a yellow solid, ^{1}H NMR (500 MHz, CDCl$_3$) δ 11.12 (1H, s), 9.76 (1H, s), 7.15 (1H, d, J = 8.5 Hz), 6.63 (1H, d, J = 8.5 Hz), 5.46 (1H, s), 3.99 (3H, s). ^{13}C NMR (125 MHz, CDCl$_3$) δ 195.2, 153.0, 149.0, 133.0, 126.1, 116.1, 103.6, 56.4.

2,3-*bis*((*tert*-Butyldimethylsilyl)oxy)-4-methoxybenzaldehyde (**7**):[49,50] 2,3-Dihydroxy-4-methoxybenzaldehyde (**6**) (1.000 g, 5.950 mmol), triethylamine (2.000 mL, 14.30 mmol) and DMAP (0.025 g, 0.200 mmol) were dissolved in dry CH$_2$Cl$_2$ (30 mL). *Tert*-butyldimethylsilyl chloride [TBSCl] (2.100 g, 13.90 mmol) was added to the reaction, which was then stirred for 18 h. Sodium bicarbonate was used to quench the reaction, which was then extracted with dicholomethane, dried with sodium sulfate, and

evaporated under reduced pressure. Flash chromatography of the crude product using a prepacked 100 g silica column [eluents: solvent A, EtOAc; solvent B, hexanes; gradient, 7% A/93% B over 1.19 min (1 CV), 7% A/93% B → 60% A/40% B over 13.12 min (10 CV), 60% A/40% B over 2.38 min (2 CV); flow rate 50.0 mL/min; monitored at λ 254 and 280 nm] yielded 2,3-*bis*((*tert*-butyldimethylsilyl)oxy)-4-methoxybenzaldehyde (**7**) (1.53 g, 3.86 mmol, 65%) as a white solid, ^{1}H NMR (500 MHz, CDCl$_3$) δ 10.23 (1H, s), 7.50 (1H, d, $J = 9$ Hz), 6.63 (1H, d, $J = 8.5$ Hz), 3.84 (3H, s), 1.05 (9H, s), 0.99 (9H, s), 0.14 (12H, s). ^{13}C NMR (125 MHz, CDCl$_3$) δ 188.9, 157.4, 150.8, 136.7, 123.3, 121.4, 105.4, 55.1, 26.1, 26.0, 18.7, 18.5, -3.9, -3.9.

(Z)-((3-Methoxy-6-(3,4,5-trimethoxystyryl)-1,2-phenylene)-*bis*(oxy))-*bis*(*tert*-butyldimethylsilane) (**9**):[49,50] Triphenyl(3,4,5-trimethoxybenzyl)phosphonium bromide (**8**) (3.20 g, 6.11 mmol) was dissolved in dry THF (100 mL) in a -10°C ice/salt bath. *N*-butyllithium (2.6 mL, 6.5 mmol, 2.5 M) was added dropwise to the reaction and the solution was subsequently stirred for 30 minutes. 2,3-*bis*((*tert*-Butyldimethylsilyl)oxy)-4-methoxybenzaldehyde (**7**) (2.000 g, 5.040 mmol) was dissolved in dry THF (10 mL) and the solution was added dropwise to the reaction, which was subsequently stirred for 5 h. Water was used to quench the reaction. Then, the reaction was then evaporated under reduced pressure. Diethyl ether was used to extract the product, which was then dried with sodium sulfate and evaporated under reduced pressure. Flash chromatography of the crude product using a prepacked 100 g silica column [eluents: solvent A, EtOAc; solvent B, hexanes; gradient, 7% A/93% B over 1.19 min (1 CV), 7% A/93% B → 40% A/60% B over 13.12 min (10 CV), 40% A/60% B over 2.38 min (2 CV); flow rate 40.0 mL/min;

monitored at λ 254 and 280 nm] yielded (*Z*)-((3-methoxy-6-(3,4,5-trimethoxystyryl)-1,2-phenylene)-*bis*(oxy))-*bis*(*tert*-butyldimethylsilane) (**9**) (1.440 g, 2.570 mmol, 70%) of the *Z*- isomer as a white solid, ^{1}H NMR (500 MHz, CDCl$_3$) δ 6.92 (1H, d, *J* = 9 Hz), 6.62 (2H, s), 6.60 (1H, d, *J* = 12 Hz), 6.37 (1H, d, *J* = 9 Hz), 6.37 (1H, d, *J* = 12 Hz), 3.83 (3H, s), 3.74 (3H, s), 3.67 (6H, s), 1.04 (9H, s), 1.00 (9H, s), 0.19 (6H, s), 0.11 (6H, s). ^{13}C NMR (125 MHz, CDCl$_3$) δ 152.7, 151.7, 136.8, 132.8, 127.7, 127.3, 123.2, 122.2, 105.9, 104.1, 60.9, 55.8, 54.9, 26.4, 26.1, 18.7, 18.6, -3.2, -3.9.

(*Z*)-2-Hydroxy-3-Methoxy-6-(3,4,5-trimethoxystyryl)benzene-1-*tert*-butyldimethylsilane (10) and (*Z*)-1-Hydroxy-3-Methoxy-6-(3,4,5-trimethoxystyryl)benzene-2-*tert*-butyldimethylsilane (11):[51] (*Z*)-((3-Methoxy-6-(3,4,5-trimethoxystyryl)-1,2-phenylene)-bis(oxy))-bis(tert-butyldimethylsilane) (**5**) (1.01 g, 1.79 mmol) was dissolved in dry THF (40 mL). Tetrabutylammonium fluoride trihydrate (1.700 g, 5.400 mmol) was added to the reaction, which was subsequently stirred for 15 min. Water was used to quench the reaction, which was then acidified with 3M HCl to pH 7, extracted with ethyl acetate, dried with sodium sulfate, and evaporated under reduced pressure. Flash chromatography of the crude product using a prepacked 100 g silica column [eluents: solvent A, EtOAc; solvent B, hexanes; gradient, 12% A/88% B over 1.19 min (1 CV), 12% A/88% B → 82% A/18% B over 13.12 min (10 CV), 82% A/18% B over 2.38 min (2 CV); flow rate 35.0 mL/min; monitored at λ 254 and 280 nm] yielded (*Z*)-2- Hydroxy-3-Methoxy-6-(3,4,5-trimethoxystyryl)benzene-1-*tert*-butyldimethylsilane (**10**) and (*Z*)-1-Hydroxy-3-Methoxy-6-(3,4,5-trimethoxystyryl)benzene-2-*tert*-butyldimethylsilane (**11**) (0.429 g, 0.882 mmol, 60%) as

a dark green solid, ^{1}H NMR (500 MHz, CDCl$_3$) δ 7.83 (2H, d, J = 9 Hz), 7.32 (2H, d, J = 8.5 Hz), 7.04 (1H, d, J = 9 Hz), 6.59 (1H, d, J = 12.5 Hz), 6.56 (1H, d, J = 12 Hz), 6.46 (2H, s), 6.27 (1H, d, J = 8.5 Hz), 3.82 (3H, s), 3.67 (6H, s), 3.50 (3H, s), 2.44 (3H, s). ^{13}C NMR (125 MHz, CDCl$_3$) δ 152.7, 147.4, 145.3, 139.3, 137.1, 135.3, 133.5, 132.1, 131.3, 129.6, 128.5, 125.7, 124.2, 120.8, 109.2, 106.1, 60.9, 56.4, 55.9, 21.7.

(Z)-3-Methoxy-2-(2-(5-nitrothiophen-2-yl)propoxy)-6-(3,4,5-trimethoxystyryl)phenyl-1-*tert*-butyldimethylsilane (12) or (Z)-3-Methoxy-1-(2-(5-nitrothiophen-2-yl)propoxy)-6-(3,4,5-trimethoxystyryl)phenyl-2-*tert*-butyldimethylsilane (13):[32] The combination of **10** and **11** (0.200 g, 0.411 mmol), DIAD (0.100 g, 0.495 mmol), and 1-(5-Nitrothiophen-2-yl)ethanol (**2**) (0.059 g, 0.34 mmol) were dissolved in dry CH$_2$Cl$_2$ (25 mL). Triphenylphosphine (0.216 g, 0.822 mmol) was added and the reaction was stirred for two days. The reaction was quenched with water, extracted with ethyl acetate, dried with sodium sulfate, and evaporated under reduced pressure. Flash chromatography of the crude product using a prepacked 100 g silica column [eluents: solvent A, EtOAc; solvent B, hexanes; gradient, 7% A/93% B over 1.19 min (1 CV), 7% A/93% B → 41% A/59% B over 8.21 min (6.9 CV), 65% A/35% B → 80%A/20%B over 1.19 min (1 CV), 80% A/10% B → 90% A/ 10% B, 90% A/ 10% B; flow rate 90.0 mL/min; monitored at λ 254 and 280 nm] yielded (Z)-3-Methoxy-2-(2-(5-nitrothiophen-2-yl)propoxy)-6-(3,4,5-trimethoxystyryl)phenyl-1-tert-butyldimethylsilane (**12**) and (Z)-3-Methoxy-1-(2-(5-nitrothiophen-2-yl)propoxy)-6-(3,4,5-trimethoxystyryl)phenyl-2-tert-butyldimethylsilane (**13**) (0.160 g, 0.249 mmol, 61%) as a yellow solid, ^{1}H NMR (500 MHz, CDCl$_3$) δ 7.84 (2H, d, J = 8.5 Hz), 7.72

(1H, d, J = 4 Hz), 7.25 (2H, d, J = 8 Hz), 6.94 (1H, d, J = 8.5 Hz), 6.75 (1H, d, J = 4.5 Hz), 6.66 (1H, d, J = 8.5 Hz), 6.48 (2H, s), 6.48 (1H, d, J = 10.5 Hz), 6.42 (1H, d, J = 12 Hz), 5.32 (1H, q, J = 6 Hz), 3.83 (3H, s), 3.80 (3H, s), 3.67 (6H, s), 1.42 (3H, d, J = 6.5 Hz). ^{13}C NMR (125 MHz, CDCl₃) δ 154.0, 152.8, 152.5, 145.1, 138.8, 134.5, 132.1, 131.7, 129.5, 128.4, 127.8, 126.1, 126.0, 124.2, 123.8, 110.3, 106.2, 75.4, 60.9, 56.1, 55.9, 21.9, 21.6, 21.5.

(Z)-3-Methoxy-2-(2-(5-nitrothiophen-2-yl)propoxy)-6-(3,4,5-trimethoxystyryl)phenol (14):[32] (Z)-3-Methoxy-2-(2-(5-nitrothiophen-2-yl)propoxy)-6-(3,4,5-trimethoxystyryl)phenyl-1-*tert*-butyldimethylsilane (**12**) (1.000 g, 1.659 mmol) and AcOH were dissolved in THF (100 mL). 2M HCl was added and the reaction was stirred for 24 h. The reaction was quenched with water, extracted with ethyl acetate, dried with sodium sulfate, and evaporated under reduced pressure. Flash chromatography of the crude product using a prepacked 100g silica column. [eluent: solvent A, EtOAc; solvent B, hexanes; gradient, 10% A/90% B over 1.19 min (1 CV), 10% A/90% B → 80% A/20% B over 13.12 min (10 CV), 80% A/20% B over 2.38 min (2 CV); flow rate 100.0 mL/min; monitored at λ 254 and 280 nm] yielded (Z)-3-Methoxy-2-(2-(5-nitrothiophen-2-yl)propoxy)-6-(3,4,5-trimethoxystyryl)phenol (**14**) (0.004 g, 0.105 mmol, 42%) as a yellow solid. ^{1}H NMR (600 MHz, CDCl₃) δ 7.78 (1H, s, J=4.2 Hz), 6.95 (1H, d, J=8.7 Hz), 6.92 (1H, d, J=4.2 Hz), 6.58 (2H, s), 6.36 (1H, d, J=8.8 Hz), 5.71 (1H, s), 5.56 (1H, q, J=6.5 Hz), 3.83 (3H, s), 3.82 (3H, s), 3.67 (6H, s), 1.72 (3H, d, J=6.5Hz). ^{13}C NMR (126 MHz, CDCl₃) δ 153.6, 152.8, 151.4, 147.5, 132.6, 132.2, 130.2, 128.2, 125.3, 123.8, 123.7, 117.5, 110.0, 105.8, 103.4, 103.3, 75.2, 60.9, 55.9, 55.8, 21.7.

Z)-3-Methoxy-2-(1-(5-nitrothiophen-2-yl)propoxy)-6-(3,4,5-trimethoxystyryl)phenol

(15):[32] (*Z*)-3-Methoxy-1-(2-(5-nitrothiophen-2-yl)propoxy)-6-(3,4,5-trimethoxystyryl)phenyl-2-*tert*-butyldimethylsilane (**13**) (1.000 g, 1.659 mmol) and AcOH were dissolved in THF (100 mL). 2M HCl was added and the reaction was stirred for 24 h. The reaction was quenched with water, extracted with ethyl acetate, dried with sodium sulfate, and evaporated under reduced pressure. Flash chromatography of the crude product using a prepacked 100g silica column. [eluent: solvent A, EtOAc; solvent B, hexanes; gradient, 15% A/85% B over 1.19 min (1 CV), 15% A/85% B → 100% A/0% B over 13.12 min (10 CV), 100% A/0% B over 2.38 min (2 CV); flow rate 25.0 mL/min; monitored at λ 254 and 280 nm] yielded *Z*)-3-Methoxy-2-(1-(5-nitrothiophen-2-yl)propoxy)-6-(3,4,5-trimethoxystyryl)phenol (**15**) (0.004 g, 0.105 mmol, 42%) as a yellow solid. ^{1}H NMR (600MHz, CDCl$_3$) δ 7.74 (1H, d, J=4.2 Hz), 6.80 (1H, d, J=8.2 Hz), 6.55 (1H, d, J=8.6 Hz), 6.54 (1H, d, J=12.4Hz), 6.47 (2H, s), 6.45 (1H, d, J=12.3 Hz), 5.71 (1H, q, J= 6.4Hz), 5.65 (1H, s), 3.87 (3H, s), 3.84 (3H, s), 3.66 (6H, s), 1.71 (3H, d, J=6.5 Hz). ^{13}C NMR (126 MHz, CDCl$_3$) δ 154.5, 152.7, 146.9, 141.6, 138.5, 137.2, 132.3, 130.2, 128.1, 125.0, 124.5, 123.7, 110.0, 106.4, 74.9, 60.9, 56.3, 55.8, 22.2.

3-((*tert*-Butyldimethylsilyl)oxy)-4-methoxybenzaldehyde (**17**):[44] Isovanillin (2.010 g, 13.20 mmol), triethylamine (4.00 mL, 28.50 mmol), and DMAP (0.045 g, 0.370 mmol) were dissolved in dry CH$_2$Cl$_2$ (60 mL). *tert*-Butyldimethylsilyl chloride (2.214 g, 14.70 mmol) was added to the reaction, which was subsequently stirred for 12 h. The reaction was quenched with water, extracted with diethyl ether, washed with water and brine,

dried with sodium sulfate, and evaporated under reduced pressure. Flash chromatography of the crude product using a prepacked 100 g silica column [eluents: solvent A, EtOAc; solvent B, hexanes; gradient, 10% A/90% B over 1.19 min (1 CV), 10% A/90% B → 27% A/73% B over 13.12 min (10 CV), 27% A/73% B over 2.38 min (2 CV); flow rate 40.0 mL/min; monitored at λ 254 and 280 nm] yielded 3-((*tert*-butyldimethylsilyl)oxy)-4-methoxybenzaldehyde (**17**) (3.17 g, 11.9 mmol, 90%) as a yellow oil, ^{1}H NMR (500 MHz, CDCl$_3$) δ 9.82 (1H, s), 7.49 (1H, dd, J = 8.5 Hz, J = 2 Hz), 7.37 (1H, d, J = 2 Hz), 6.96 (1H, d, J = 8.5 Hz), 3.90 (3H, s), 1.00 (9H, s), 0.17 (6H, s). ^{13}C NMR (125 MHz, CDCl$_3$) δ 190.9, 156.6, 130.2, 126.3, 120.0, 111.1, 55.6, 25.6, 18.4, -4.6.

(3-((*tert*-Butyldimethylsilyl)oxy)-4-methoxyphenyl)(3,4,5-trimethoxyphenyl)methanol (19):[44] 1-Bromo-3,4,5-trimethoxybenzene (1.810 g, 7.310 mmol) was dissolved in dry THF (60 mL) in a dry ice/acetone bath at -78 °C. *N*-butyllithium (2.8 mL, 7.0 mmol, 2.5 M) was added dropwise to the reaction, which was subsequently stirred for 30 minutes. 3-((*tert*-Butyldimethylsilyl)oxy)-4-methoxybenzaldehyde (2.000 g, 7.500 mmol) was dissolved in dry THF (20 mL) and the solution was added dropwise. The reaction was subsequently stirred for 5 h. The reaction was quenched with water, acidified to pH 7 with 3 M HCl, extracted with diethyl ether, washed with water and brine, dried with sodium sulfate, and evaporated under reduced pressure. Flash chromatography of the crude product using a prepacked 100 g silica column [eluents: solvent A, EtOAc; solvent B, hexanes; gradient, 10% A/90% B over 1.19 min (1 CV), 10% A/90% B → 80% A/20% B over 13.12 min (10 CV), 80% A/20% B over 2.38 min (2 CV); flow rate 40.0 mL/min; monitored at λ 254 and 280 nm] yielded

(3-((*tert*-butyldimethylsilyl)oxy)-4-methoxyphenyl)(3,4,5-trimethoxyphenyl)methanol

(**19**) (2.02 g, 4.65 mmol, 62%) as a pale yellow oil, ^{1}H NMR (500 MHz, CDCl$_3$) δ 6.89

(2H, m), 6.80 (1H, d, J = 8.5 Hz), 6.57 (2H, d, J = 4.5 Hz), 5.24 (1H, d, J = 4.5 Hz), 3.81

(3H, s), 3.77 (9H, s), 0.94 (9H, d, J = 3.5 Hz), 0.11 (6H, d, J = 2.5 Hz). ^{13}C (125 MHz,

CDCl$_3$) δ 153.0, 150.3, 144.7, 140.0, 136.5, 119.9, 119.4, 111.8, 103.4, 75.5, 60.7, 55.9,

55.5, 25.7, 18.4, -4.6.

(3-((*tert*-Butyldimethylsilyl)oxy)-4-methoxyphenyl)(3,4,5-

trimethoxyphenyl)methanone (20):[44] (3-((*tert*-Butyldimethylsilyl)oxy)-4-

methoxyphenyl)(3,4,5-trimethoxyphenyl)methanol (**19**) (3.000 g, 6.900 mmol), Celite

(2.450 g, 0.00004 mmol), and potassium carbonate [K$_2$CO$_3$] (2.460 g, 17.80 mmol) were

dissolved in dry CH$_2$Cl$_2$ (130 mL) in an ice bath at 0 °C. Pyridinium chlorochromate

[PCC] (1.52 g, 7.04 mmol) was added in small increments and the reaction was stirred for

18 h. The reaction was filtered with CH$_2$Cl$_2$ in a frit funnel containing a 50/50 mixture of

Celite and silica gel then evaporated under reduced pressure. Flash chromatography of

the crude product using a prepacked 100 g silica column [eluents: solvent A, EtOAc;

solvent B, hexanes; gradient, 10% A/90% B over 1.19 min (1 CV), 10% A/90% B →

45% A/55% B over 13.12 min (10 CV), 45% A/55% B over 2.38 min (2 CV); flow rate

40.0 mL/min; monitored at λ 254 and 280 nm] yielded (3-((*tert*-butyldimethylsilyl)oxy)-

4-methoxyphenyl)(3,4,5-trimethoxyphenyl)methanone (**20**) (1.790 g, 4.140 mmol, 60%)

as a yellow oil, ^{1}H NMR (500 MHz, CDCl$_3$) δ 7.40 (1H, d, J = 8 Hz), 7.33 (1H, s), 6.99

(2H, s), 6.87 (1H, d, J = 8.5 Hz), 3.88 (3H, s), 3.84 (3H, s), 3,83 (6H, s), 0.96 (9H, s),

0.14 (6H, s). ^{13}C NMR (125 MHz, CDCl$_3$) δ 194.5, 154.9, 152.7, 144.6, 141.5, 133.3, 130.4, 125.3, 110.7, 107.4, 60.9, 56.2, 55.5, 25.6, 18.4, -4.6.

Phenstatin (21):[44] (3-((*tert*-Butyldimethylsilyl)oxy)-4-methoxyphenyl)(3,4,5-trimethoxyphenyl)methanone (**20**) (3.590 g, 8.310 mmol) was dissolved in dry THF (100 mL). Tetrabutylammonium fluoride trihydrate (3.930 g, 12.50 mmol) was added and the reaction was stirred for 18 h. The reaction was quenched with water, acidified to pH 7 with 3 M HCl, extracted with ethyl acetate, dried with sodium sulfate, and evaporated under reduced pressure. Flash chromatography of the crude product using a prepacked 100 g silica column [eluents: solvent A, EtOAc; solvent B, hexanes; gradient, 12% A/88% B over 1.19 min (1 CV), 12% A/88% B → 99% A/1% B over 13.12 min (10 CV), 99% A/1% B over 2.38 min (2 CV); flow rate 40.0 mL/min; monitored at λ 254 and 280 nm] yielded phenstatin (**21**) (2.06 g, 6.47 mmol, 71%) as a white solid, ^{1}H NMR (500 MHz, CDCl$_3$) δ 7.42 (1H, s), 7.37 (1H, d, J = 8.5 Hz). 7.01 (2H, s), 6.90 (1H, d, J = 8 Hz), 3.94 (3H, s), 3.90 (3H, s), 3.85 (6H, s). ^{13}C NMR (125 MHz, CDCl$_3$) δ 194.7, 152.8, 150.2, 145.3, 141.6, 133.1, 131.0, 123.7, 116.2, 110.0, 109.7, 107.5, 61.0, 56.3, 56.1.

(4-Methoxy-3-((2-(5-nitrothiophen-2-yl)propan-2-yl)oxy)phenyl)(3,4,5-trimethoxyphenyl)methanone (22):[44] Phenstatin (0.405 g, 1.270 mmol), ADDP (0.289 g, 1.430 mmol), and 1-(5-Nitrothiophen-2-yl)Propan-2-ol (**4**) (0.454 g, 2.850 mmol) were dissolved in dry CH$_2$Cl$_2$ (40 mL). Tributylphosphine (0.574 g, 2.190 mmol) was added and the reaction was stirred for two days. The reaction was quenched with water, extracted with ethyl acetate, dried with sodium sulfate, and evaporated under reduced

pressure. Flash chromatography of the crude product using a prepacked 25 g silica column [eluents: solvent A, EtOAc; solvent B, hexanes; gradient, 10% A/90% B over 1.19 min (1 CV), 10% A/90% B → 80% A/20% B over 13.12 min (10 CV), 80% A/20% B over 2.38 min (2 CV); flow rate 50.0 mL/min; monitored at λ 254 and 280 nm] yielded (4-methoxy-3-((5-nitrothiophen-2-yl)methoxy)phenyl)(3,4,5-trimethoxyphenyl)methanone **(43)** (0.198 g, 0.431 mmol, 34%) as a brown solid, ^{1}H NMR (500 MHz, CDCl$_3$) δ 7.83 (1H, d, J = 4.5 Hz), 7.51 (1H, d, J = 1.5 Hz), 7.49 (1H, dd, J = 8 Hz, J = 1.5 Hz), 7.06 (1H, d, J = 4.5), 6.99 (2H, s), 6.97 (1H, d, J = 8.5 Hz), 5.33 (2H, s), 3.98 (3H, s), 3.93 (3H, s), 3.87 (6H, s). ^{13}C NMR (125 MHz, CDCl$_3$) δ 194.3, 153.7, 152.8, 147.7, 146.9, 141.7, 133.0, 130.2, 128.4, 126.6, 125.2, 115.5, 110.6, 107.4, 66.3, 61.0, 56.3, 56.2.

CHAPTER FOUR

Conclusions

This study has achieved the synthesis of CA1 BAPCs with the *mono*methyl trigger attached and a phenstatin BAPC with the *geminal-di*methyl trigger attached. *Tert*-butyldimethylsilyl chloride [TBSCl] has shown to be a good protecting group at either the C-2 or C-3 position of CA1 and at the C-3 position of phenstatin in order to mask the polar characteristic of the hydroxyl group so that it does not interfere with the Wittig and halogen-metal exchange reactions, or the Mitsunobu reaction on CA1. Therefore, the *mono*methyl trigger was attached either at the C-2 or C-3 position of the protected CA1. Tetra-*N*-butylammonium fluoride [TBAF] is a good deprotecting method for CA1 and phenstatin. The *Z*-isomer of CA1 has shown to be difficult to isolate because of the marked similarity in polarity to the *E* isomer. Usually, the Mitsunobu reaction occurs in the order of adding alcohol 1, ADDP, and alcohol 2.[52] However, that order gives a low yield in this study. Thus, an alternative order has been performed such that alcohol 1, ADDP, and alcohol 2 were mixed together first, then the tributylphosphine was added second. As a result, the phenstatin and CA1 BAPCs were obtained in better yields. The future of this research would be to synthesize CA1 BAPCs with dimethyl triggers and phenstatin BAPCs with monomethyl trigger, and to evaluate their cytotoxicity against cancer cell lines under normoxic and hypoxic conditions in collaboration with the Trawick Laboratory.

REFERENCES CITED

(1) Siemann, D. W. The Unique Characteristics of Tumor Vasculature and Preclinical Evidence for Its Selective Disruption by Tumor-Vascular Disrupting Agents. *Cancer Treat. Rev.* **2011**, *37* (1), 63–74.

(2) Brown, J. M.; Wilson, W. R. Exploiting Tumour Hypoxia in Cancer Treatment. *Nat. Rev. Cancer* **2004**, *4* (6), 437–447.

(3) Siemann, D. W.; Bibby, M. C.; Dark, G. G.; Dicker, A. P.; Eskens, F. A. L. M.; Horsman, M. R.; Marmé, D.; Lorusso, P. M. Differentiation and Definition of Vascular-Targeted Therapies. *Clin. Cancer Res. Off. J. Am. Assoc. Cancer Res.* **2005**, *11* (2 Pt 1), 416–420.

(4) Siemann, D. W. *Vascular-Targeted Therapies in Oncology*; J. Wiley: Chichester, West Sussex ; Hoboken, NJ, 2006.

(5) Mason, R. P.; Zhao, D.; Liu, L.; Trawick, M. L.; Pinney, K. G. A Perspective on Vascular Disrupting Agents That Interact with Tubulin: Preclinical Tumor Imaging and Biological Assessment. *Integr. Biol.* **2011**, *3* (4), 375–387.

(6) Ferrara, N.; Hillan, K. J.; Novotny, W. Bevacizumab (Avastin), a Humanized Anti-VEGF Monoclonal Antibody for Cancer Therapy. *Biochem. Biophys. Res. Commun.* **2005**, *333* (2), 328–335.

(7) Lee, R. M.; Gewirtz, D. A. Colchicine Site Inhibitors of Microtubule Integrity as Vascular Disrupting Agents. *Drug Dev. Res.* **2008**, *69* (6), 352–358.

(8) Kim, C.; Yang, H.; Fukushima, Y.; Saw, P. E.; Lee, J.; Park, J.-S.; Park, I.; Jung, J.; Kataoka, H.; Lee, D.; Heo, W. D.; Kim, I.; Jon, S.; Adams, R. H.; Nishikawa, S.-I.; Uemura, A.; Koh, G. Y. Vascular RhoJ Is an Effective and Selective Target for Tumor Angiogenesis and Vascular Disruption. *Cancer Cell* **2014**, *25* (1), 102–117.

(9) Hamel, E.; Lin, C. M. Stabilization of the Colchicine-Binding Activity of Tubulin by Organic Acids. *Biochim. Biophys. Acta BBA - Gen. Subj.* **1981**, *675* (2), 226–231.

(10) Dumontet, C.; Jordan, M. A. Microtubule-Binding Agents: A Dynamic Field of Cancer Therapeutics. *Nat. Rev. Drug Discov.* **2010**, *9* (10), 790–803.

(11) Dumontet, C.; Jordan, M. A. Microtubule-Binding Agents: A Dynamic Field of Cancer Therapeutics. *Nat. Rev. Drug Discov.* **2010**, *9* (10), 790–803.

(12) Lee, R. M.; Gewirtz, D. A. Colchicine Site Inhibitors of Microtubule Integrity as Vascular Disrupting Agents. *Drug Dev. Res.* **2008**, *69* (6), 352–358.

(13) Boyland, E.; Boyland, M. E. Studies in Tissue Metabolism. *Biochem. J.* **1937**, *31* (3), 454–460.

(14) Strecker, T. E.; Odutola, S. O.; Lopez, R.; Cooper, M. S.; Tidmore, J. K.; Charlton-Sevcik, A. K.; Li, L.; MacDonough, M. T.; Hadimani, M. B.; Ghatak, A.; Liu, L.; Chaplin, D. J.; Mason, R. P.; Pinney, K. G.; Trawick, M. L. The Vascular Disrupting Activity of OXi8006 in Endothelial Cells and Its Phosphate Prodrug OXi8007 in Breast Tumor Xenografts. *Cancer Lett.* **2015**, *369* (1), 229–241.

(15) Schlaepfer, D. D.; Hauck, C. R.; Sieg, D. J. Signaling through Focal Adhesion Kinase. *Prog. Biophys. Mol. Biol.* **1999**, *71* (3–4), 435–478.

(16) Ridley, A. J.; Hall, A. The Small GTP-Binding Protein Rho Regulates the Assembly of Focal Adhesions and Actin Stress Fibers in Response to Growth Factors. *Cell* **1992**, *70* (3), 389–399.

(17) Ren, X.-D.; Kiosses, W. B.; Sieg, D. J.; Otey, C. .; Schlaepfer, D. D.; Schwartz, M. . Focal Adhesion Kinase Suppresses Rho Activity to Promote Focal Adhesion. *J. Cell Sci.* **2000**, *113* (20), 3673–3678.

(18) Sastry, S. K.; Burridge, K. Focal Adhesions: A Nexus for Intracellular Signaling and Cytoskeletal Dynamics. *Exp. Cell Res.* **2000**, *261* (1), 25–36.

(19) Amano, M.; Ito, M.; Kimura, K.; Fukata, Y.; Chihara, K.; Nakano, T.; Matsuura, Y.; Kaibuchi, K. Phosphorylation and Activation of Myosin by Rho-Associated Kinase (Rho-Kinase). *J. Biol. Chem.* **1996**, *271* (34), 20246–20249.

(20) Sandquist, J. C.; Swenson, K. I.; DeMali, K. A.; Burridge, K.; Means, A. R. Rho Kinase Differentially Regulates Phosphorylation of Nonmuscle Myosin II Isoforms A and B during Cell Rounding and Migration. *J. Biol. Chem.* **2006**, *281* (47), 35873–35883.

(21) Tozer, G. M.; Kanthou, C.; Baguley, B. C. Disrupting Tumour Blood Vessels. *Nat. Rev. Cancer* **2005**, *5* (6), 423–435.

(22) Wilson, W. R.; Hay, M. P. Targeting Hypoxia in Cancer Therapy. *Nat. Rev. Cancer* **2011**, *11* (6), 393–410.

(23) Huttunen, K. M.; Raunio, H.; Rautio, J. Prodrugs—from Serendipity to Rational Design. *Pharmacol. Rev.* **2011**, *63* (3), 750–771.

(24) Guise, C. P.; Mowday, A. M.; Ashoorzadeh, A.; Yuan, R.; Lin, W.-H.; Wu, D.-H.; Smaill, J. B.; Patterson, A. V.; Ding, K. Bioreductive Prodrugs as Cancer Therapeutics: Targeting Tumor Hypoxia. *Chin. J. Cancer* **2014**, *33* (2), 80–86.

(25) Phillips, R. M. Targeting the Hypoxic Fraction of Tumours Using Hypoxia-Activated Prodrugs. *Cancer Chemother. Pharmacol.* **2016**, *77* (3), 441–457.

(26) Jameson, M. B.; Rischin, D.; Pegram, M.; Gutheil, J.; Patterson, A. V.; Denny, W. A.; Wilson, W. R. A Phase I Trial of PR-104, a Nitrogen Mustard Prodrug Activated by Both Hypoxia and Aldo-Keto Reductase 1C3, in Patients with Solid Tumors. *Cancer Chemother. Pharmacol.* **2010**, *65* (4), 791–801.

(27) Konopleva, M.; Thall, P. F.; Yi, C. A.; Borthakur, G.; Coveler, A.; Bueso-Ramos, C.; Benito, J.; Konoplev, S.; Gu, Y.; Ravandi, F.; Jabbour, E.; Faderl, S.; Thomas, D.; Cortes, J.; Kadia, T.; Kornblau, S.; Daver, N.; Pemmaraju, N.; Nguyen, H. Q.; Feliu, J.; Lu, H.; Wei, C.; Wilson, W. R.; Melink, T. J.; Gutheil, J. C.; Andreeff, M.; Estey, E. H.; Kantarjian, H. Phase I/II Study of the Hypoxia-Activated Prodrug PR104 in Refractory/relapsed Acute Myeloid Leukemia and Acute Lymphoblastic Leukemia. *Haematologica* **2015**, *100* (7), 927–934.

(28) Ortiz de Montellano, P. R. Cytochrome P450-Activated Prodrugs. *Future Med. Chem.* **2013**, *5* (2), 213–228.

(29) Gu, Y.; Guise, C. P.; Patel, K.; Abbattista, M. R.; Li, J.; Lie, J.; Sun, X.; Atwell, G. J.; Boyd, M.; Patterson, A. V.; Wilson, W. R. Reductive Metabolism of the

Dinitrobenzamide Mustard Anticancer Prodrug PR-104 in Mice. *Cancer Chemother. Pharmacol.* **2011**, *67* (3), 543–555.

(30) Patterson, A. V.; Ferry, D. M.; Edmunds, S. J.; Gu, Y.; Singleton, R. S.; Patel, K.; Pullen, S. M.; Hicks, K. O.; Syddall, S. P.; Atwell, G. J.; Yang, S.; Denny, W. A.; Wilson, W. R. Mechanism of Action and Preclinical Antitumor Activity of the Novel Hypoxia-Activated DNA Cross-Linking Agent PR-104. *Clin. Cancer Res. Off. J. Am. Assoc. Cancer Res.* **2007**, *13* (13), 3922–3932.

(31) Khan, S.; O'Brien, P. J. Molecular Mechanisms of Tirapazamine (SR 4233, Win 59075)-Induced Hepatocyte Toxicity under Low Oxygen Concentrations. *Br. J. Cancer* **1995**, *71* (4), 780–785.

(32) Thomson, P.; Naylor, M. A.; Everett, S. A.; Stratford, M. R. L.; Lewis, G.; Hill, S.; Patel, K. B.; Wardman, P.; Davis, P. D. Synthesis and Biological Properties of Bioreductively Targeted Nitrothienyl Prodrugs of Combretastatin A-4. *Mol. Cancer Ther.* **2006**, *5* (11), 2886–2894.

(33) Rischin, D.; Peters, L. J.; O'Sullivan, B.; Giralt, J.; Fisher, R.; Yuen, K.; Trotti, A.; Bernier, J.; Bourhis, J.; Ringash, J.; Henke, M.; Kenny, L. Tirapazamine, Cisplatin, and Radiation versus Cisplatin and Radiation for Advanced Squamous Cell Carcinoma of the Head and Neck (TROG 02.02, HeadSTART): A Phase III Trial of the Trans-Tasman Radiation Oncology Group. *J. Clin. Oncol. Off. J. Am. Soc. Clin. Oncol.* **2010**, *28* (18), 2989–2995.

(34) Pettit, G. R.; Singh, S. B.; Niven, M. L.; Hamel, E.; Schmidt, J. M. Isolation, Structure, and Synthesis of Combretastatins A-1 and B-1, Potent New Inhibitors of Microtubule Assembly, Derived from Combretum Caffrum. *J. Nat. Prod.* **1987**, *50* (1), 119–131.

(35) Pettit, G. R.; Singh, S. B.; Hamel, E.; Lin, C. M.; Alberts, D. S.; Garcia-Kendall, D. Isolation and Structure of the Strong Cell Growth and Tubulin Inhibitor Combretastatin A-4. *Experientia* **1989**, *45* (2), 209–211.

(36) D'Amato, R. J.; Lin, C. M.; Flynn, E.; Folkman, J.; Hamel, E. 2-Methoxyestradiol, an Endogenous Mammalian Metabolite, Inhibits Tubulin Polymerization by Interacting at the Colchicine Site. *Proc. Natl. Acad. Sci. U. S. A.* **1994**, *91* (9), 3964–3968.

(37) Pettit, G. R.; Lippert, J. W. Antineoplastic Agents 429. Syntheses of the Combretastatin A-1 and Combretastatin B-1 Prodrugs. *Anticancer. Drug Des.* **2000**, *15* (3), 203–126.

(38) Rustin, G.; Galbraith, S.; Anderson, H.; Stratford, M. R. L.; Folkes, L.; Sena, L.; Gumbrell, L.; Price, P. M. Phase I Clinical Trial of Weekly Combretstatin A4 Phosphate: Clinical and Pharmacokinetic Results. *J. Clin. Oncol. Off. J. Am. Soc. Clin. Oncol.* **2003**, *21* (15), 2815.

(39) PCC + Bevacizumab + CA4P Versus PCC + Bevacizumab + Placebo for Subjects With Platinum Resistant Ovarian Cancer - Full Text View - ClinicalTrials.gov https://clinicaltrials.gov/ct2/show/study/NCT02641639 (accessed Apr 22, 2016).

(40) A Phase I Clinical Trial of OXi4503 for Relapsed and Refractory AML and MDS - Full Text View - ClinicalTrials.gov (accessed Mar 20, 2016).

(41) Safety Study of Increasing Doses of Combretasatin A1 Diphosphate (OXi4503) as Monotherapy in Subjects With Hepatic Tumor Burden - Tabular View - ClinicalTrials.gov (accessed Mar 20, 2016).

(42) Pettit, G. R.; Toki, B.; Herald, D. L.; Verdier-Pinard, P.; Boyd, M. R.; Hamel, E.; Pettit, R. K. Antineoplastic Agents. 379. Synthesis of Phenstatin Phosphate1a,. *J. Med. Chem.* **1998**, *41* (10), 1688–1695.

(43) Paolo Lupattelli, M. D. A Novel Approach to Combretastatins: From trans-Epoxide to CA-4 and Its Dioxolane Derivative. *Eur. J. Org. Chem.* **2008**, *2009* (1), 141–145.

(44) Kamal, A.; Kumar, G. B.; Vishnuvardhan, M. V. P. S.; Shaik, A. B.; Reddy, V. S.; Mahesh, R.; Sayeeda, I. B.; Kapure, J. S. Synthesis of Phenstatin/isocombretastatin–chalcone Conjugates as Potent Tubulin Polymerization Inhibitors and Mitochondrial Apoptotic Inducers. *Org Biomol Chem* **2015**, *13* (13), 3963–3981.

(45) Vichai, V.; Kirtikara, K. Sulforhodamine B Colorimetric Assay for Cytotoxicity Screening. *Nat. Protoc.* **2006**, *1* (3), 1112–1116.

(46) Devkota, L.; Lin, C.-M.; Strecker, T. E.; Wang, Y.; Tidmore, J. K.; Chen, Z.; Guddneppanavar, R.; Jelinek, C. J.; Lopez, R.; Liu, L.; Hamel, E.; Mason, R. P.; Chaplin, D. J.; Trawick, M. L.; Pinney, K. G. Design, Synthesis, and Biological Evaluation of Water-Soluble Amino Acid Prodrug Conjugates Derived from Combretastatin, Dihydronaphthalene, and Benzosuberene-Based Parent Vascular Disrupting Agents. *Bioorg. Med. Chem.* **2016**, *24* (5), 938–956.

(47) Siles, R.; Ackley, J. F.; Hadimani, M. B.; Hall, J. J.; Mugabe, B. E.; Guddneppanavar, R.; Monk, K. A.; Chapuis, J.-C.; Pettit, G. R.; Chaplin, D. J.; Edvardsen, K.; Trawick, M. L.; Garner, C. M.; Pinney, K. G. Combretastatin Dinitrogen-Substituted Stilbene Analogues as Tubulin-Binding and Vascular-Disrupting Agents. *J. Nat. Prod.* **2008**, *71* (3), 313–320.

(48) Thomson, P.; Naylor, M. A.; Everett, S. A.; Stratford, M. R. L.; Lewis, G.; Hill, S.; Patel, K. B.; Wardman, P.; Davis, P. D. Synthesis and Biological Properties of Bioreductively Targeted Nitrothienyl Prodrugs of Combretastatin A-4. *Mol. Cancer Ther.* **2006**, *5* (11), 2886–2894.

(49) Tanpure, R. P.; Strecker, T. E.; Chaplin, D. J.; Siim, B. G.; Trawick, M. L.; Pinney, K. G. Regio- and Stereospecific Synthesis of Mono-β- d -Glucuronic Acid Derivatives of Combretastatin A-1. *J. Nat. Prod.* **2010**, *73* (6), 1093–1101.

(50) Tanpure, R. P.; Nguyen, B. L.; Strecker, T. E.; Aguirre, S.; Sharma, S.; Chaplin, D. J.; Siim, B. G.; Hamel, E.; Lippert, J. W.; Pettit, G. R.; Trawick, M. L.; Pinney, K. G. Regioselective Synthesis of Water-Soluble Monophosphate Derivatives of Combretastatin A-1. *J. Nat. Prod.* **2011**, *74* (7), 1568–1574.

(51) Patterson, L. H.; McKeown, S. R. AQ4N: A New Approach to Hypoxia-Activated Cancer Chemotherapy. *Br. J. Cancer* **2000**, *83* (12), 1589–1593.

(52) Mitsunobu, O.; Yamada, M. Preparation of Esters of Carboxylic and Phosphoric Acid via Quaternary Phosphonium Salts. *Bull. Chem. Soc. Jpn.* **1967**, *40* (10), 2380–2382.